Observations of the step-like accelerating processes of cold ions in the reconnection layer at the dayside magnetopause

Article

Accepted Version

Accepted Manuscript

Article

Observations of the step-like accelerating processes of cold ions in the reconnection layer at the dayside magnetopause

Qing-He Zhang, Michael Lockwood, John C. Foster, Qiu-Gang Zong, Malcolm W. Dunlop, Shun-Rong Zhang, Jøran Moen, Bei-Chen Zhang

PII:	S2095-9273(18)30003-3
DOI:	https://doi.org/10.1016/j.scib.2018.01.003
Reference:	SCIB 308

To appear in: *Science Bulletin*

Please cite this article as: Q-H. Zhang, M. Lockwood, J.C. Foster, Q-G. Zong, M.W. Dunlop, S-R. Zhang, J. Moen, B-C. Zhang, Observations of the step-like accelerating processes of cold ions in the reconnection layer at the dayside magnetopause, *Science Bulletin* (2018), doi: https://doi.org/10.1016/j.scib.2018.01.003

Observations of the step-like accelerating processes of cold ions in the reconnection layer at the dayside magnetopause

Qing-He Zhang[a,*], Michael Lockwood[b], John C. Foster[c], Qiu-Gang Zong[d], Malcolm W. Dunlop[e], Shun-Rong Zhang[c], Jøran Moen[f], Bei-Chen Zhang[g]

[a] *Shandong Provincial Key Laboratory of Optical Astronomy and Solar-Terrestrial Environment, Institute of Space Sciences, Shandong University, Weihai, Shandong, 264209, China.*

[b] *Department of Meteorology, University of Reading, Earley Gate, Post Office Box 243, RG6 6BB, UK.*

[c] *MIT Haystack Observatory, Westford, MA 01886, USA*

[d] *School of Earth and Space Sciences, Peking University, Beijing,10087, China*

[e] *Space Sciences Division, SSTD, Rutherford Appleton Laboratory, Didcot, OX11 0QX,UK*

[f] *Department of Physics, University of Oslo, Blindern, 0316, Oslo, Norway*

[g] *SOA Key Laboratory for Polar Science, Polar Research Institute of China, Shanghai,200136, China*

*** Contact Author:** Qing-He Zhang

Institute of Space Sciences, Shandong University,

NO. 180 Wenhua Xilu, Weihai, Shandong, 264209, China

Tel: +86-631-5672210 Fax: +86-631-5685054

E-mail: zhangqinghe@sdu.edu.cn

Abstract

Cold ions of plasmaspheric origin have been observed to abundantly appear in the magnetospheric side of the Earth's magnetopause. These cold ions could affect the magnetic reconnection processes at the magnetopause by changing the Alfvén velocity and the reconnection rate, while they could also be heated in the reconnection layer during the ongoing reconnections. We report *in situ* observations from a partially crossing of a reconnection layer near the subsolar magnetopause. During this crossing, step-like accelerating processes of the cold ions were clearly observed, suggesting that the inflow cold ions may be separately accelerated by the rotation discontinuity and slow shock inside the reconnection layer.

Key words: cold ions, magnetic reconnection, ions acceleration of ions, magnetopause

Introduction

Cold ions (few eV) of plasmaspheric origin are often observed in the outer magnetosphere and the magnetospheric side of magnetopause, which are in the form of drainage plumes mainly driven there by convection electric field during the high geomagnetic activity [1-7], and are carried there by plasmaspheric wind via combinational consequence of corotation and convection electric field during quiet geomagnetic activity [6-11]. Cold ions from the polar ionosphere can also directly reach the dayside magnetopause along the magnetic field lines via outflow [12]. When the cold ions reach the dayside magnetopause, they may be involved in, and influenced by, magnetic reconnection in the magnetopause current sheet [5,13-17]. On reaching the magnetopause, it has long been thought to be lost to interplanetary space as the field lines are opened by reconnection [13, 18-22].

The operation of MR is expected to result in a reconnection layer with characteristic ion and electron diffusion regions and an X-line of the central, null (zero) field and associated bundles of reconnected flux (flux tubes, moving in predictable ways from the magnetic merging line) during periods of ongoing or intermittent reconnection [23-27]. Previous theories and simulations predicted that there are several boundaries within the reconnection layer, which can accelerate the ions at the associated area [28, 29]. Different models, however, predicted different boundaries [28, 29]. In the ideal MHD simulation, rotational discontinuities (RD), slow shocks or slow expansion fan (SS/SEF), and contact discontinuity (CD) are present in the reconnection layer [28], while in the hybrid simulation, the contact discontinuity cannot be identified due to the mixing of ions from the magnetosheath and magnetosphere, and slow shocks and slow expansion waves are modified [29]. At the magnetopause, the Alfvén wave is an intermediate wave or shock and transmitted through RD, thus, people often talk about RD and Alfvén wave together [30]. Observations confirmed the existence of the RDs and SS/SEF [31, 32]. Recent laboratory experiments and particle-in-cell simulations also suggested that the Hall effects can produce a strong electric field in the reconnection plane that is strongest across the separatrices, which separates the incoming field line region from the exhaust of reconnected field lines [33, 34]. Dipolarization fronts and flux ropes in the reconnection region of the magnetotail can also accelerate the particles, especially the electrons [35-39]. Clear separated acceleration signatures are difficult, despite recent access to multi-point sampling on small and meso-scale, owing to the fact that most of the encounters are highly dynamic. We report here one of the first, clear partial transitions through a reconnection layer near the subsolar magnetopause, which shows clear accelerations of the cold ions in the reconnection layer.

Observations and Results

Figure 1 summarizes conditions on 17 January 2013, where the IMF and solar wind data come from the NASA OMNIWeb and has been shifted 5 minutes from the nose of bow shock to the subsolar dayside magnetopause**.** The IMF was steadily southward after 17:00

UT ($B_z \approx -10$nT), the solar wind dynamic pressure was initially typical ($P_{SW} \approx 5$nPa) but then fell to unusually low values (≈ 0.1nPa) (Fig. 1a and b). We have projected polar maps of ionospheric total electron into the equatorial plane using the same procedure as in Walsh et al. [40] (except a more adaptive magnetic field model [41] and magnetopause model [42] were used – see supplementary materials). This procedure has been used to compare the storm enhanced density (SED) plumes identified at low altitudes GPS total electron content (TEC) map with the plasmaspheric drainage plume determined by EUV imaging from the IMAGE spacecraft [43], and with the in situ plasma observations by THEMIS (Time History of Events and Macroscale Interactions during Substorms mission [44]) satellites [40], which indicated that SED plumes are associated with the erosion of the outer plasmasphere (plasmaspheric plume) by strong sub-auroral polarization stream (SAPS) electric fields [43, 45]. Figure 1(c) is a keogram of the mapped TEC from the noon meridian as a function of time. Early in the time period, the high-density plasma plume from the dusk plasmasphere contacted the near-noon magnetopause but this was not the case later in the period (see also extended data in supplementary materials). The blue line in Fig. 1(c) is the inbound pass of spacecraft E of the THEMIS mission, which was close to the noon-midnight meridian and subsolar region (Fig. 1d and e). The mapping used in Walsh et al. [40] assumed that density variations in the topside ionosphere form fully field-aligned structures that map all the way to the equatorial plane. If this assumption is valid, THEMIS-E should have detected ionospheric plasma just inside the magnetopause during this pass. Figure 2 not only confirms that this was the case, it tells us about the subsequent evolution of this plasma.

THEMIS-E first encountered energetic magnetospheric ions (see Fig. 2e at energy $E \approx 10^4$eV) around 18:17:50 and the magnetosheath current sheet at 18:21:50 (see Fig. 2a) when B_L turns positive and the bipolar FTE signature in B_N is seen [40]. What we identify as accelerated ionospheric ions (see below) were first seen at 18:22:30 (Fig. 2e at E< 100 eV) causing the ion density N_i to be larger than even in the magnetosheath (Fig. 2b). Later, (18:28:30-18:29:50, 18:36:10-18:38:10 and 18:46:50-18:47:50) periods of closed field lines deep in the plasmasheet (where ion temperature T_i is high and N_i low) were encountered, readily identified in Fig. 2(b) and 2(c). Between the first two of these periods the satellite returned to the reconnection layer (the regions between the two separatrices of the reconnection) and observed a variable mixture of magnetosheath and magnetospheric plasma, however between the second two, the spacecraft remained in the magnetosphere and saw un-accelerated ionospheric ions (E < 20eV in Fig. 2e), which caused N_i to rise but T_i to fall without any sheath plasma being present. Thus THEMIS-E was seeing the arrival of the low energy plasma as Fig. 1(c) predicts it should.

There are some small intervals in these data that prove the putative ionospheric plasma in the reconnection layer does indeed come from the unaccelerated population seen in the outer magnetosphere. The first of these was a brief entry into an accelerated flow region near 18:30 (when V_L briefly reached 180 kms^{-1}), the second around 18:38:35 (when Fig. 2d shows V_L reached 100 kms^{-1}). Figure 2(g)-2(l) concentrate on the second of these events. At 18:35:35 THEMIS-E observed a sharp transition from magnetosheath-dominated to magnetosphere-dominated plasma (Fig.2k and Fig.2l). There is no current sheet but a weak indication of accelerated flow in V_L. After this, the ionospheric component was seen at E < 20eV but then weakened. The persistent negative V_N component (roughly approximate V_X in GSM coordinates, Fig.2j) reveals that this was caused by inward motion of the magnetopause. At 18:37:30, V_N was further negative, and this in-out motion of the magnetopause briefly returned the satellite to the reconnection layer. Figure 2(g) shows that the satellite crossed the current sheet twice (characterized by B_L components change the sign twice around 18:38:00 UT) with a strong guide field (B_M component). Figure 2(k) shows that low-energy ionospheric plasma was step-like accelerated up to about 80eV and shows a

Formatted: Font color: Auto

reverse "U" type structure with steps around 18:38:30 UT before the sequence was reversed on the way out of the event. The accelerated flow had a peak magnitude of $V_L \approx 100$ kms^{-1} which corresponds to 63 eV energy for protons and hence the observed energy is consistent with the derived velocity moment (which assumes the ions detected were protons). The continuous energy increase on the way into and decrease on the way out of this event proves that the lower-energy ions in the accelerated flow region came from the ionospheric population seen in the magnetosphere near the magnetopause. The lack of any such dispersion for the higher energy ions seen during the event (E ≈ 500 eV) shows they came from the magnetosheath due to the reconnection. The magnetosheath ions reached the spacecraft at about 18:38:27 UT (ion edge) and disappeared after about 18:38:45 UT (ion edge). The electron edge, first observation of magnetosheath electrons, is observed at about 18:38:24 and 18:39:24 UT, which was referred as the separatrix of the reconnection layer [46, 47]. It is worth noting that the time duration between the latter electron and ion edges encountering was much longer than the former ones, which may be because the reconnection layer was slow down (the ion velocity clearly decreased (Fig. 2j)) and made THEMIS E stay much longer between the latter electron and ion edges.

Discussions

Figure 2(k) shows a reverse "U" type structure with steps for the low-energy ionospheric plasma around 18:38:30 UT. What happened there when the spacecraft crossed the magnetopause boundary? Vaivads et al. [46] suggested that there is an Alfvén edge or RD between the electron and ion edges on the mangetospheric side of the current sheet. From Fig. 2, we have identified two electron edges at about 18:38:24 and 18:39:24 UT, and two ion edges at about 18:38:27 and 18:38:45UT, respectively. If there is RD between electron and ion edges, we should observe clear rotations of the magnetic field when the spacecraft

Formatted: Font color: Auto

Formatted: Font color: Auto

Formatted: Font color: Auto

Formatted: Font color: Auto

Formatted: Font color: Auto

crossed the RD. We have plotted the 3D magnetic field vectors along the orbit tracks of THEMIS E for the interval of 18:38:00-18:39:30 UT (Fig. 3a). From Figure 3a, we can find the magnetic field was main in northward at the beginning, but started to rotate earthward and duskward at about 18:38:25 UT, and then gradually rotated back from about 18:38:33 UT. These rotations of the magnetic field suggested there are RDs during this crossing. We also have performed a Walén test for the interval of 18:38:19-18:39:35 UT and found there is a good de-Hoffman-Teller (HT) frame for this reconnection layer with a velocity (V_{HT}) of 278.16 km/s and [-0.49, -0.01, 0.87] in GSE coordinates and a well Walén relation with a slope of 0.98 between the Alfvén velocity and the residual plasma velocity in the HT frame (Fig. 3b). These suggest that there was an RD at the magnetospheric side of the reconnection layer indeed. Ideal MHD simulation suggested that the ratio of upstream and downstream magnetic field can be used to identify that the discontinuity is a slow shock or slow expansion fan by using the following equation [28, 31].

$$\eta=(B_{t2}/B_{t1})=\{1+\beta(1-P_2/P_1)\}^{1/2}$$

where B_t is the discontinuity tangential magnetic field and P is particle pressure, and subscripts 1 and 2 represent to upstream and downstream of the discontinuity. For a slow shock (SS), $\eta<1$, and for a slow expansion fan, $\eta>1$, [28, 31]. In our case, the P_1 is about 0.02 nPa and P_2 is about 0.14 nPa, and the mean plasma $\beta=2P\mu_0/B^2 \approx 0.13$, which gives $\eta \approx 0.47$ and suggests this discontinuity is a slow shock. The basic characteristics of slow shocks are that the magnetic fields are refracted towards the shock normal with a decrease of their tangential component and total strength when the shock front passed them [28, 48]. In our case, the magnetic field was refracted towards shock normal which is roughly antiparallel to the boundary normal **n** due to the magnetopause inward motion during the interval of interest, and the trangential component (roughly B_L) and total strength of the magnetic field all decreased (Fig. 2 and Fig. 3a). Thus, these calculations and observations

Formatted: Font color: Auto

Formatted: Font color: Auto

Formatted: Font color: Auto

Formatted: Font color: Auto

Formatted: Font color: Auto

Formatted: Font color: Auto

Formatted: Font color: Auto

suggest that there were RD and SS been observed indeed when THEMIS E partially crossed the reconnection layer. These are consistent with the time elapsed since reconnection of the given field lines crossed.

Ion accelerations often occurred due to the dispersion of phase-steepened Alfvén wave and/or through shock drift acceleration or diffusion shock acceleration when they crossed an RD or SS [49]. Thus, the reverse "U" type structure in the low-energy ionospheric ions seen by THEMIS-E suggests that these ions were step-like accelerated by the boundaries within the reconnection layer, when the THEMIS-E crossed the separatrix, RD and SS on the magnetospheric side and the SS on the magnetosheath side, respectively (Fig. 4). The energy of the ions also seems step-like decrease when the spacecraft moved back and crossed these boundaries again to the magnetosphere due to the sunward and northward motion of the reconnection layer (schematic shown in Fig. 4). Although the 3s time resolution of the THEMIS data may trend to make the ion spectrum looks stepped, it still can clearly show that the accelerations associated with the boundaries within the reconnection layer make the ion energy sharply increase in a very short time interval.

To escape the magnetosphere, ions must reach beyond the tail reconnection site before the re-closure of magnetic field lines (as for the red trajectory in Fig.5). These ions will not receive as much (or any) of the Coriolis acceleration experienced by ions rising from the low-altitude cleft ion fountain source [50-52]. They are likely to be accelerated if the field line catches them up due to increased Alfvén speed at the magnetopause with increasingly negative *X*. The combined data clearly demonstrate a path for ionospheric plasma, collected in the outer plasmasphere, to enter into accelerated flow along the magnetopause driven by magnetic reconnection. All ion species in this region would have the velocity V_L of 100 kms^{-1} near along the field line, but is this adequate for escape? The data on this day provide an estimate of how long the field lines remain open. At ionospheric heights, the ionization tongue breaks up into polar cap patches and the TEC maps allow us to follow their evolution [53,54]. It has been shown [53, 54] that patches only escape the nightside polar cap and move onto sunward-convecting closed field lines when the field lines are reclosed in the tail. On the day studied here, as shown in Zhang et al. [53], this yields at least 2 hours before open field lines are reclosed. By then, if the accelerated ionospheric ions keep their velocity and move along the field lines, they would have moved at least 113 R_E ($100 \times 2 \times 3600 / 6370 \approx 113 R_E$), placing them at $X < -93$ R_E down the tail (allowing for $20R_E$ around the dayside magnetopause). Most estimates of even distant reconnection sites are at $X >> -90$ R_E. It is therefore almost certain that the ionospheric ions seen here reaching the dayside magnetopause and being accelerated by reconnection did escape the magnetosphere. Thus, detached plasmaspheric plasma reaching a dayside magnetopause reconnection site would be very efficient at expelling large fluxes of ionospheric plasma into interplanetary space (schematic shown in Fig.5), if these plasmas gain enough energy (acceleration) and keep their velocity moving along the field lines. Because the GPS observations used here are routinely available, this opens up a genuine possibility of monitoring the loss of atmospheric material via this mechanism on a continuous basis and studying its variations with season and solar wind conditions.

Conclusions

Cold ions of plasmaspheric plume have been observed both in the projected GPS TEC data and in the *in situ* plasma data from THEMIS satellite near the dayside magnetopause. THEMIS-E partially crossed a reconnection layer near the subsolar magnetopause and clearly observed step-like accelerating processes of these cold ions. The observations suggest that the inflow cold ions may be separately accelerated by the rotation discontinuity (or Alfvén wave) and slow shock inside the reconnection layer.

Formatted: Font color: Auto

Acknowledgments: This work in China was supported by the National Natural Science Foundation (41574138, 41604139) and the Shandong Provincial Natural Science Foundation (JQ201412). The work at Reading University was supported by STFC consolidated grant ST/M000885/1. The Norwegian contribution was supported by the Research Council of Norway grant 230996. S.R.Z. acknowledges support from the U.S. NASA LWS project NNX15AB83G and the U.S. DoD MURI project ONR15-FOA- 0011. MIT Haystack GPS data acquisition (http://madrigal. haystack.mit.edu/madrigal/), led by A. J. Coster, is supported by the U.S. NSF Geospace Facility program under an agreement AGS-1242204 with Massachusetts Institute of Technology. We acknowledge NASA contract NAS5-02099 and V. Angelopoulos for use of data from the THEMIS Mission. The authors also wish to thank the International Space Science Institute in Beijing (ISSI-BJ) for supporting and hosting the meetings of the International Team on "Multiple-instrument observations and simulations of the dynamical processes associated with polar cap patches/aurora and their associated scintillations", during which the discussions leading/contributing to this publication were initiated/held.

References

1. Borovsky JE, Denton MH. A statistical look at plasmaspheric drainage plumes. J Geophys Res 2008; 113: A09221.
2. Moore T, Fok MC, Delcourt D, et al. Plasma plume circulation and impact in an MHD substorm. J Geophys Res 2008; 113: A06219.
3. Darrouzet F, Keyser JD, Décréau P, et al. Statistical analysis of plasmaspheric plumes with cluster/whisper observations. Ann Geophys 2008; 26: 2403–2417.
4. Darrouzet, F, Gallagher DL, André N, et al. Plasmaspheric density structures and dynamics: Properties observed by the cluster and image missions. In: Darrouzet F, De Keyser J, Pierrard V, editors. The Earth's Plasmasphere. Netherlands: Springer; 2009, p. 55–106.
5. Walsh B, Phan T, Sibeck D, et al. The plasmaspheric plume and magnetopause reconnection. Geophys Res Lett 2014; 41: 223–228.
6. Fu HS, Tu J, Song P, et al. The nightside-to-dayside evolution of the inner magnetosphere: Imager for Magnetopause-to-Aurora Global Exploration Radio Plasma Imager observations. J Geophys Res 2010; 115: A04213.
7. Fu HS, Tu J, Cao JB, et al. IMAGE and DMSP observations of a density trough inside the plasmasphere. J Geophys Res 2010; 115: A07227.
8. Matsui H, Mukai T, Ohtani S, et al. Cold dense plasma in the outer magnetosphere. J Geophys Res 1999; 104(A11): 25,077–25,095.
9. André N, Lemaire J. Convective instabilities in the plasmasphere. J Atmos Sol Terr Phys 2006; 68(2): 213–227.
10. Tu J, Song P, Reinisch BW, et al. Smooth electron density transition from plasmasphere to the subauroral region. J Geophys Res 2007; 112: A05227.

11. Dandouras I. Detection of a plasmaspheric wind in the Earth's magnetosphere by the cluster spacecraft. Ann Geophys 2013; 31: 1143–1153.

12. Lee SH, Zhang H, Zong QG, et al. Asymmetric ionospheric outflow observed at the dayside magnetopause. J Geophys Res Space Physics 2015; 120: 3564–3573.

13. Su YJ, Borovsky JE, Thomsen MF, et al. Plasmaspheric material at the reconnecting magnetopause. J Geophys Res 2000; 105: 7591-7600.

14. McFadden J, Carlson C, Larson D, et al. Structure of plasmaspheric plumes and their participation in magnetopause reconnection: First results from THEMIS. Geophys Res Lett 2008; 35: L17S10.

15. André M, Vaivads A, Khotyaintsev YV, et al. Magnetic reconnection and cold plasma at the magnetopause. Geophys Res Lett 2010; 37: L22108.

16. Lee JH, Angelopoulos V. On the presence and properties of cold ions near Earth's equatorial magnetosphere. J Geophys Res Space Physics 2014; 119:1749–1770.

17. Toledo-Redondo S, Vaivads A, André M, et al. Modification of the hall physics in magnetic reconnection due to cold ions at the Earth's magnetopause. Geophys Res Lett 2015; 42: 6146–6154.

18. Elphic RC., Thomsen MF, Borovsky JE. The fate of the outer plasmasphere. Geophys Res Lett 1997; 24: 365-368.

19. Fuselier SA, Klumpar DM, Shelley EG. Ion reflection and transmission during reconnection at the Earth's subsolar magnetopause. Geophys Res Lett 1991; 18: 139-142.

20. Freeman JW, Hills HK, Hill TW, et al. Heavy ion circulation in the Earth's magnetosphere. Geophys Res Lett 1977; 4: 195-197.

21. Gosling JT, Thomsen MF, Bame SJ, et al. Cold ion beams in the low latitude boundary layer during accelerated flow events. Geophys Res Lett 1990; 17: 2245-2248.

22. Su YJ, Borovsky JE, Thomsen MF, et al. Plasmaspheric material on high-latitude open field lines. J Geophys Res 2001; 106: 6085-6095.

23. Dungey JW. Interplanetary magnetic field and the auroral zones. Phys Rev Lett 1961; 6: 47–48.

24. Dunlop MW, Zhang QH, Bogdanova YV, et al. Extended magnetic reconnection across the dayside magnetopause. Phys Rev Letts 2011; 107: 025004.

25. Fu HS, Vaivads A, Khotyaintsev YV, et al. Intermittent energy dissipation by turbulent reconnection. Geophys Res Lett 2017; 44: 37–43.

26. Huang SY, Zhou M, Sahraoui F, et al. Wave properties in the magnetic reconnection diffusion region with high β: Application of the k-filtering method to Cluster multispacecraft data. J Geophys Res 2010; 115: A12211.

27. Huang SY, Zhou M, Sahraoui F, et al. Observations of turbulence within reconnection jet in the presence of guide field. Geophys Res Lett 2012; 39: L11104.

28. Heyn MF, Biernat HK, Rijnbeek RP, et al. The structure of reconnection layers. J Plasma Physics 1988; 40(2): 235-252.

29. Lin Y, Lee LC. Formation of the magnetopause boundary layer by magnetic reconnection. Adv Space Res 1995; 15(8/9): 531-535.

30. Lee LC. Transmission of Alfvén waves through the rotational discontinuity at magnetopause. Planetary and Space Sci 1982; 30 (11): 1127-1132.

31. Lockwood M, Hapgood MA. On the Cause of a Magnetospheric Flux Transfer Event. J Geophys Res 1998; 103: 26453-26478.

32. Zhang QH, Dunlop MW, Lockwood M, et al. Inner plasma structure of the low-latitude reconnection layer. J Geophys Res 2012; 117: A08205.

33. Yamada, M., Yoo J, Jara-Almonte J, et al. Conversion of magnetic energy in the

magnetic reconnection layer of a laboratory plasma. Nat Commun 2014; 5:4774.

34. Lu Q, Huang C, Xie J, et al. Features of separatrix regions in magnetic reconnection: Comparison of 2-D particle-in-cell simulations and Cluster observations. J Geophys Res 2010; 115: A11208.

35. Zhou M, Deng X, Ashour-Abdalla M, et al. Cluster observations of kinetic structures and electron acceleration within a dynamic plasma bubble. J Geophys Res Space Physics 2013; 118: 674–684.

36. Huang SY, Zhou M, Deng XH, et al. Kinetic structure and wave properties associated with sharp dipolarization front observed by Cluster. Ann Geophys 2012; 30: 97-107.

37. Huang SY, Vaivads A, Khotyaintsev YV, et al. Electron Acceleration in the Reconnection Diffusion Region: Cluster Observations. Geophys Res Lett 2012; 39: L11103.

38. Huang SY, Retino A, Phan TD, et al. In situ observations of flux rope at the separatrix region of magnetic reconnection. J Geophys Res Space Physics 2016; 121: 205–213.

39. Huang SY, Sahraoui F, Retino A, et al. MMS observations of ion-scale magnetic island in the magnetosheath turbulent plasma. Geophys Res Lett 2016; 43: 7850-7858.

40. Walsh BM, Foster JC, Erickson PJ, et al. Simultaneous Ground- and Space-Based Observations of the Plasmaspheric Plume and Reconnection. Science 2014; 343: 1122-1125.

41. Tsyganenko NA, Stern DP. Modeling the global magnetic field of the large-scale Birkeland current systems. J Geophys Res 1996; 101: 27187-27198.

42. Shue JH, Song P, Russell CT, et al. Magnetopause location under extreme solar wind conditions. J Geophys Res 1998; 103: 17691-17700.

43. Foster JC, Erickson PJ, Coster AJ, et al. Ionospheric signatures of plasmaspheric tails.

Geophys Res Lett 2002; 29:1-4.

44. Angelopoulos V. The THEMIS mission. Space Sci Rev 2008; 141: 453– 476.
45. Foster JC, Coster AJ, Erickson PJ, et al. Stormtime observations of the flux of plasmaspheric ions to the dayside cusp/magnetopause. Geophys Res Lett 2004; 31: L08809.
46. Vaivads A, Retinò A, Khotyaintsev YV, et al. The Alfvén edge in asymmetric reconnection. Ann Geophys 2010; 28: 1327-1331.
47. Toledo-Redondo S, André M, Vaivads A, et al. Cold ion heating at the dayside magnetopause during magnetic reconnection. Geophys Res Lett 2016; 43: 58–66.
48. De Moortel I, Galsgaard K. Numerical modelling of 3D reconnection due to rotational footpoint motions. A&A 2006; 451: 1101-1115.
49. Tsurutani BT, Lakhina GS, Pickett JS, et al. Nonlinear Alfve´n waves, discontinuities, proton perpendicular acceleration, and magnetic holes/decreases in interplanetary space and the magnetosphere: intermediate shocks? Nonlinear Processes in Geophysics 2005; 12: 321–336.
50. Cladis JB. Parallel acceleration and transport of ions from polar ionosphere to plasma sheet. Geophys Res Lett 1986; 13: 893-896.
51. Lockwood M, Waite JJH, Moore TE, et al. A new source of suprathermal O+ ions near the dayside polar cap boundary. J Geophys Res1985; 90: 4099-4116.
52. Lockwood M, Chandler MO, Horwitz JL, et al. The cleft ion fountain. J Geophys Res 1985; 90: 9736-9748.
53. Zhang QH, Zhang BC, Lockwood M, et al. Direct Observations of the Evolution of Polar Cap Ionization Patches. Science 2013; 339: 1597-1600.
54. Zhang QH, Lockwood M, Foster JC, et al. Direct observations of the full Dungey

convection cycle in the polar ionosphere for southward interplanetary magnetic field conditions, J Geophys Res Space Physics 2015; 120: 4519–4530.

Figure Captions:

Fig. 1. (Color online) Data from 17 January 2013. (a) The interplanetary magnetic field X, Z and Y components (in the GSM frame). (b) The solar wind dynamic pressure PSW. (c) A keogram showing total electron content mapped from the noon meridian to the equatorial plane using the Tsyganenko T96 model [41], as a function of time. The black line shows the magnetopause position from a different model [42] and the blue line the path of THEMIS-E. (d) and (e) The orbit tracks of THEMIS-E relative to the modelled magnetopause position in XZ_{GSE} and XY_{GSE} plane (GSE is geocentric solar ecliptic coordinate system).

Fig. 2. (Color online) THEMIS-E spacecraft data for (a-f) 18:10-18:50 and (g-l) detail of 18:35-18:40. Fields and flows are shown in magnetopause (MP) aligned "LMN" coordinates during the time interval around the MP crossing of the spacecraft (about 18:38:07-18:38:32 UT), where N is the magnetopause normal, L is in the (Z_{GSM}, N) plane and M completes a left-handed set (GSM is the geocentric solar magnetic coordinate system) with **l** = (0.77，-0.03，0.64), **m** = (-0.63，0.14，0.76) and **n** = (0.11, 0.99, -0.09) in GSM coordinates. (a and g) Magnetic field components (B_L, B_M and B_N in blue, green and red); (b and h) ion density, N_i; (c and i) ion temperature, T_i; (d and j) ion velocities (V_L, V_M and V_N in blue, green and red); (e and k) and (f and l) ion and electron energy-time spectrogram of differential energy flux for all pitch angles, respectively. The associated regions, crossed by the spacecraft, are presented as horizontal thick color lines with labels below panels f and l.

Fig. 3. (Color online) A 3D plot of the magnetic field data and a Walén test of plasma data measured by THEMIS E. (a) The 3D magnetic field vectors in GSE coordinates along the orbit tracks of THEMIS E for the interval of 18:38:00-18:39:30 UT. The vectors have been separated and colored every 30 seconds. The blue and magenta vectors (with arrows) present the directions of deHoffmann-Teller frame velocity (V_{HT}) and the mean boundary normal n. (b) A Walén test of the reconnection layer crossing for the interval of 18:38:19-18:39:35 UT.

The colored dots represent the three components of the velocity in GSE coordinates (Red for V_X, green for V_Y, and blue for V_Z).

Fig. 4. (Color online) Schematics of the structure of the reconnection layer and the acceleration processes of the ions on the trajectory of the spacecraft. An asymmetrical reconnection layer is often seen on the dayside magnetopause since the plasma and magnetic field parameters are different in the magnetosphere (Msp) and magnetosheath (Msh).

Fig. 5. (Color online) Schematics of ionospheric ion outflow. The X direction, from the centre of the Earth to the centre of the Sun, is to the left. The brown line is the outer boundary of the magnetosphere, the magnetopause, inside which are three distinct regions: the tail lobes (black) contain “open” magnetic field lines that thread the magnetopause which are generated in the Dungey cycle during periods of southward IMF by magnetic reconnection at the dayside magnetopause (at the yellow dot) and re-closed by reconnection in the tail (at the red dot) [23]. The plasmasheet (dark grey) contains closed field lines which connect the ionospheres in the two hemispheres and never thread the magnetopause. Closed field lines convect sunward in the Dungey cycle. The plasmasphere (in white) is also on closed field lines and has higher plasma densities than the plasmasheet because magnetic flux tube volumes are smaller and can be filled by outflows from the ionosphere. The coloured lines show trajectories for ions of plasmaspheric origin from reconnection acceleration region (see text). Note that all ions are moving along the magnetic field lines but trajectories are not field-aligned because the field lines move as part of the Dungey convection cycle. Higher energy ion trajectories (red arrows) are closer to field aligned than lower energy ones (in mauve) because they have higher field parallel velocity.

408

Field Code Changed

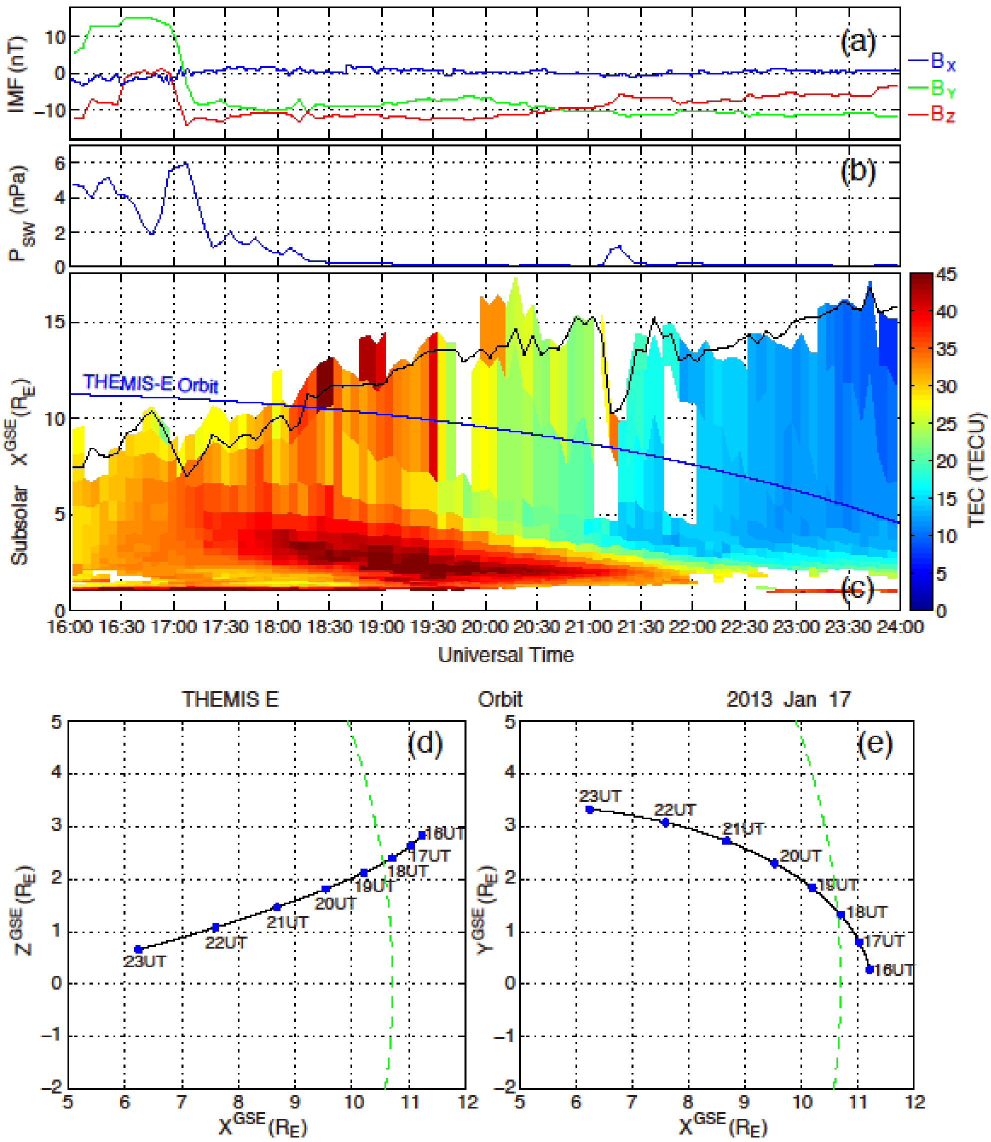

Field Code Changed

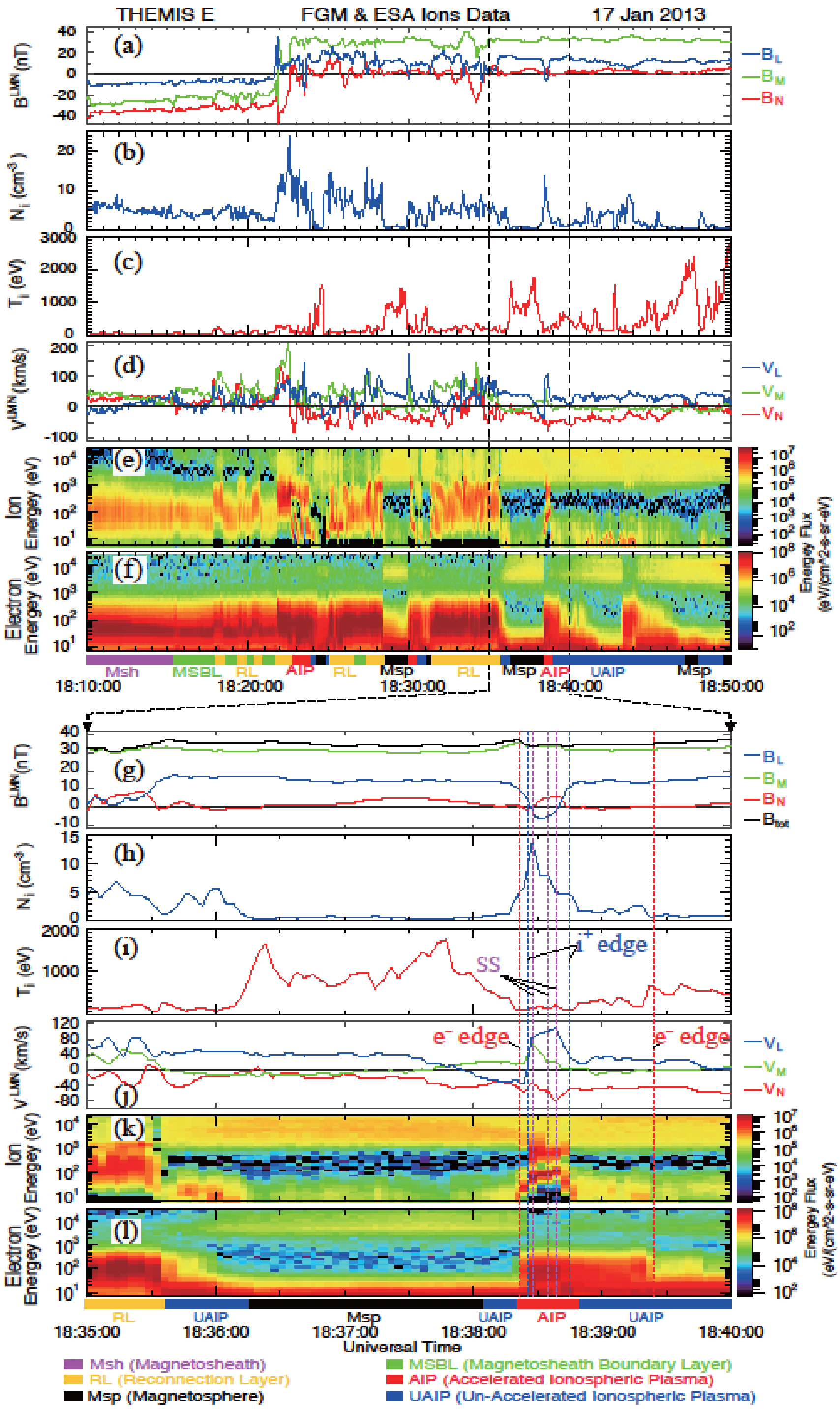

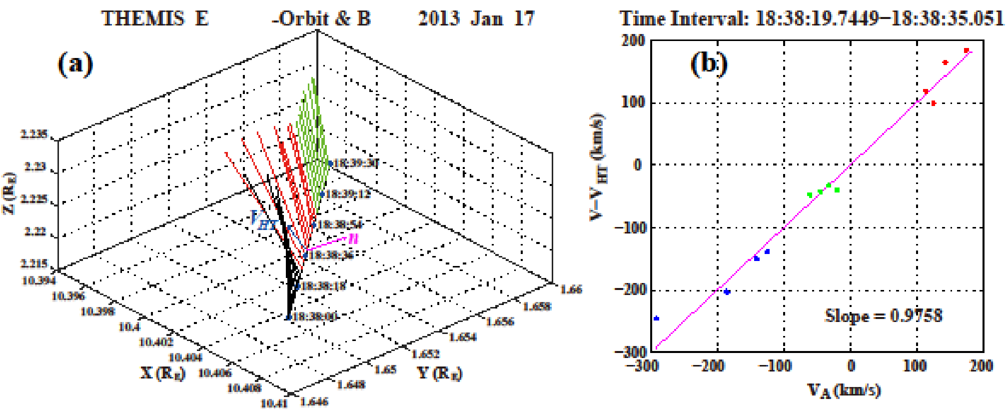
THEMIS E -Orbit & B 2013 Jan 17
(a)
Z (R_E)
X (R_E)
Y (R_E)
18:39:30
18:39:12
18:38:54
18:38:36
18:38:18
18:38:00
Time Interval: 18:38:19.7449−18:38:35.051
(b)
V−V_HT (km/s)
V_A (km/s)
Slope = 0.9758

Field Code Changed

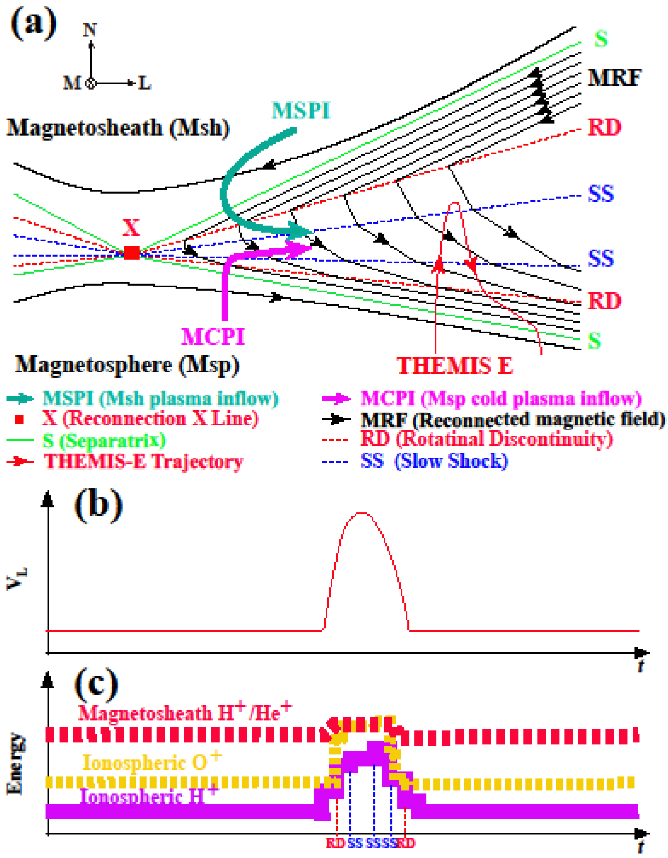

415

416

Field Code Changed